

Supporting Figures

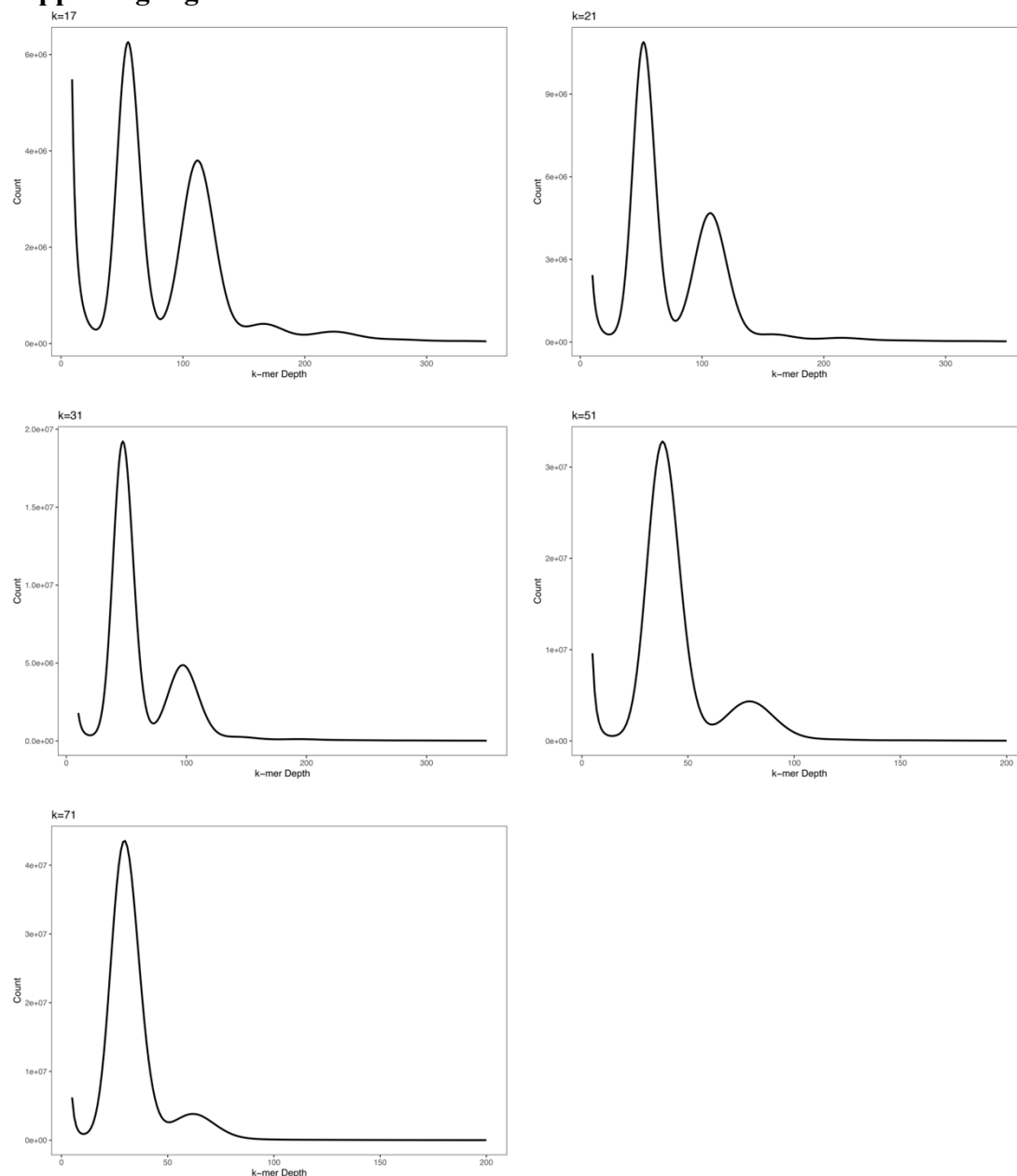


Figure S1 K-mer based genome size estimates. K = 17, 21, 31, 51 and 71 count histograms of Illumina paired-end sequence data for tetraploid *Trapa natans*. These plots were used to estimate genome size (total k-mer number)/(peak depth). K = 17: a total of 50,029,871,544 17-mers were detected with a peak depth of 54 and an estimated genome size of 926.48 Mb; K = 21: a total of 51,476,584,112 21-mers were detected with a peak depth of 52 and an estimated genome size of 989.93 Mb; K = 31: a total of 50,607,610,875 31-mers were detected with a peak depth of 47 and an estimated genome size of 1076.76 Mb; K = 51: a total of 43,270,633,852 51-mers were detected with a peak depth of 38 and an estimated genome size of 1138.70 Mb; K = 71: a total of 34,807,248,461 71-mers were detected with a peak depth of 30 and an estimated genome size of 1160.24 Mb.

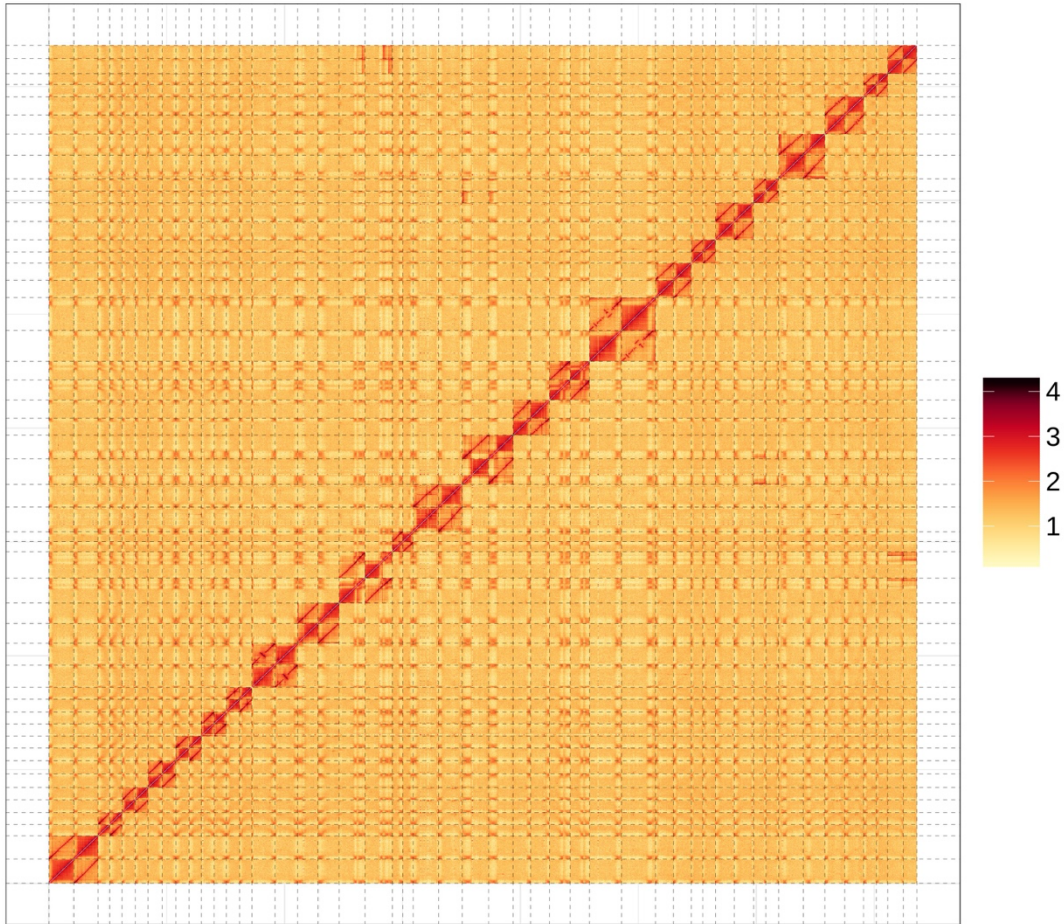


Figure S2 Genome-wide analysis of chromatin interactions in the tetraploid *Trapa natans* genome based on Hi-C data.

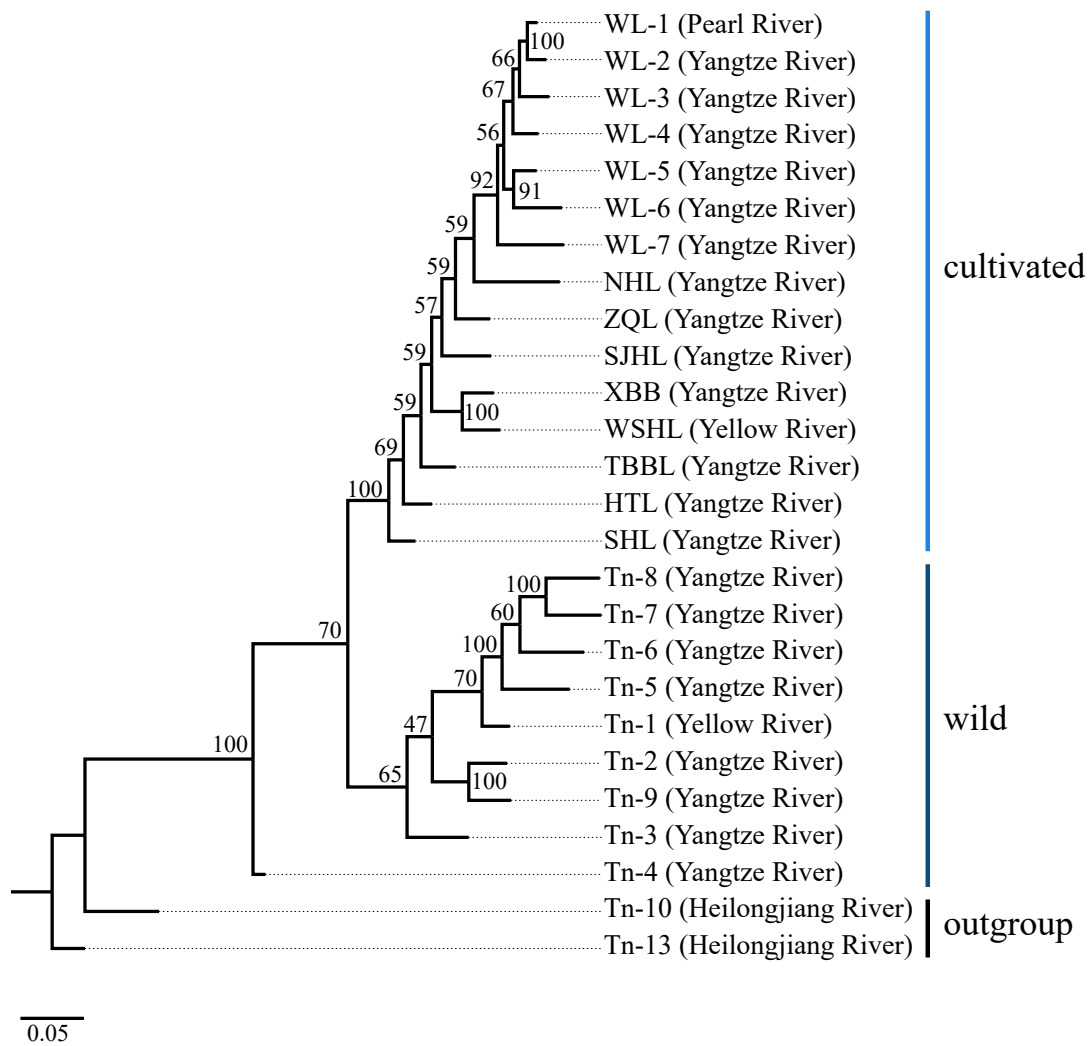


Figure S3 Phylogenetic relationships of diploid *Trapa natans* (2x, AA) from the PYY region inferred from maximum likelihood (ML) analysis based on SNP data.

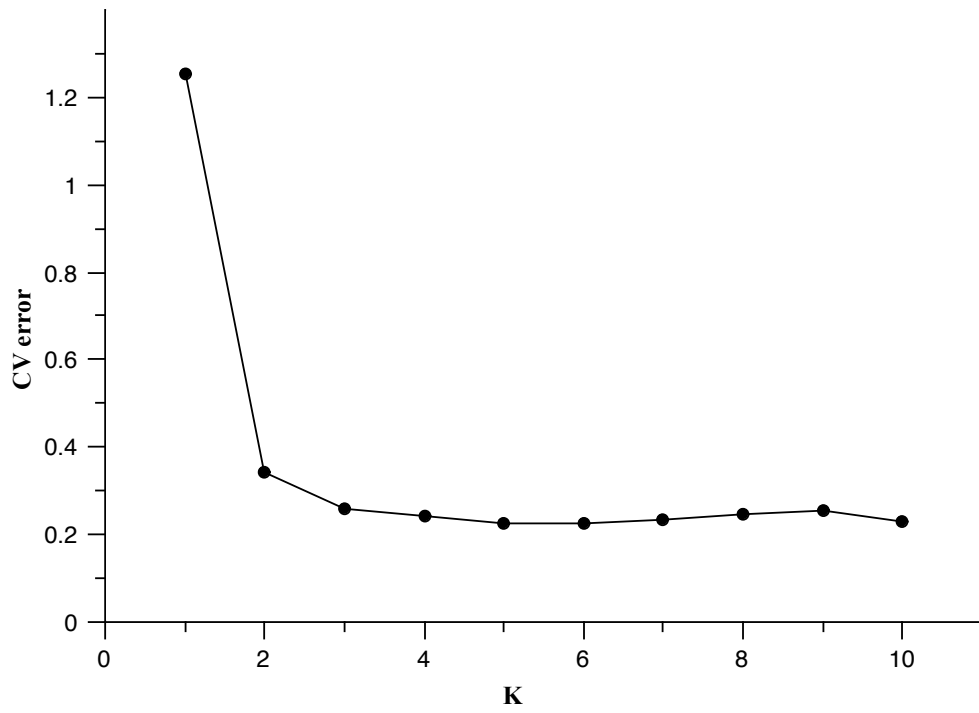


Figure S4 Plot of ADMIXTURE cross-validation error across values of K.

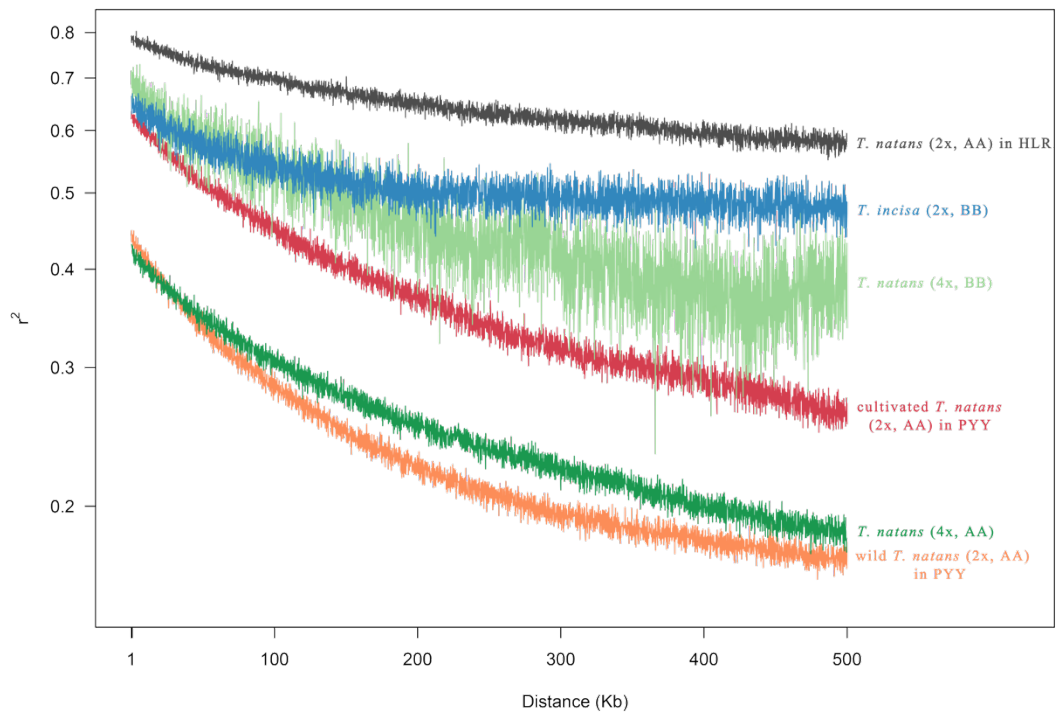


Figure S5 LD decay determined by correlation of allele frequencies (r^2) against distance (kb) in six *Trapa* populations. Note that the A and B subgenomes of tetraploid *T. natans* individuals were treated separately (4x, AA vs. BB). PYY, Pearl-Yangtze-Yellow River region; HLR, Heilongjiang River region.

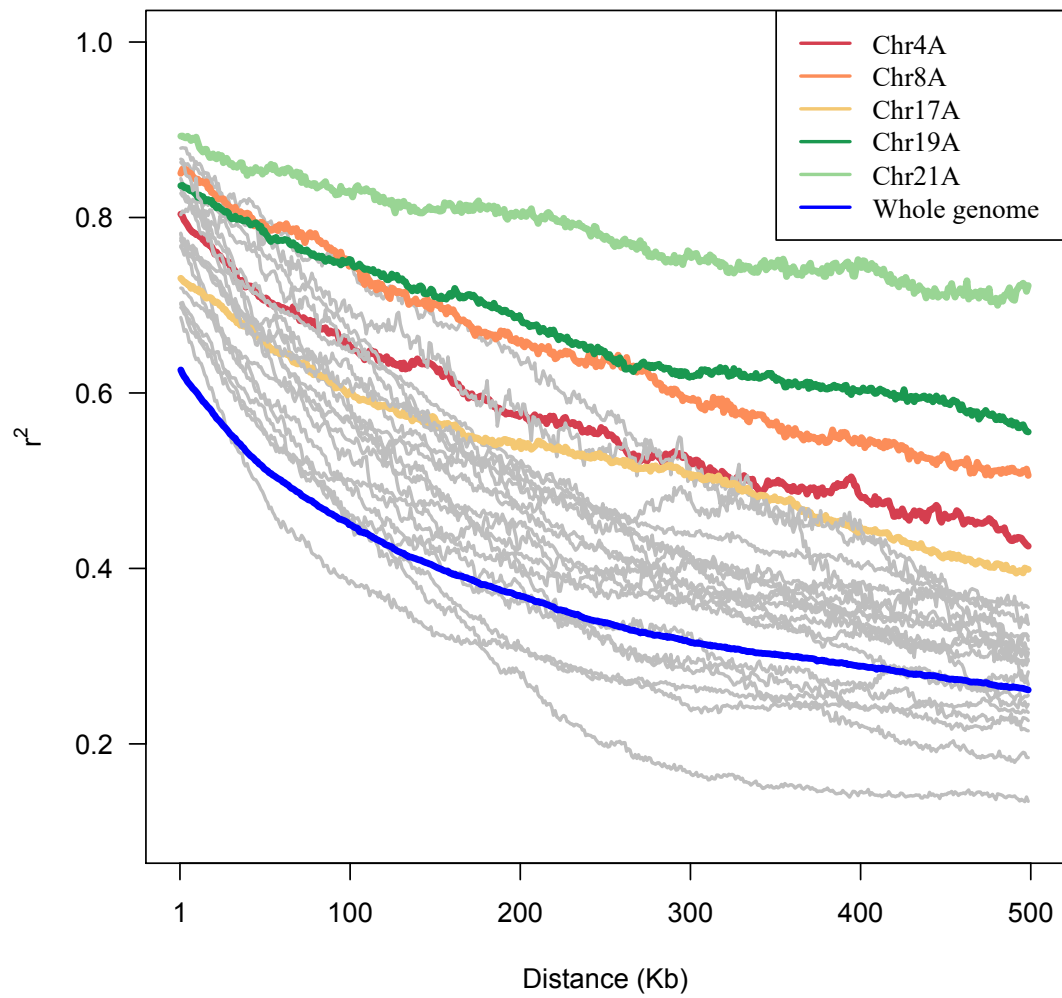


Figure S6 LD decay distances in cultivars of *Trapa natans* for each of the 24 chromosomes.

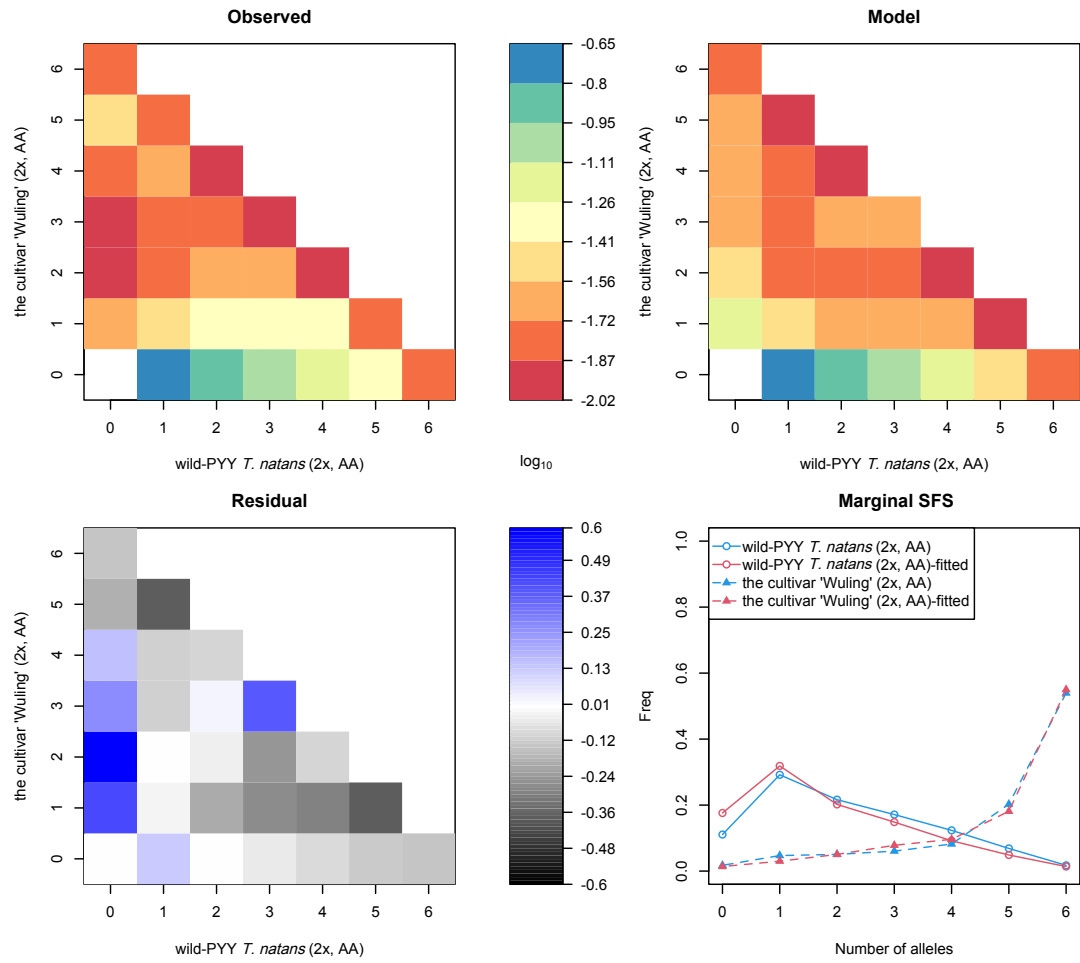


Figure S7 The goodness-of-fit of the best scenario summarized by the observed 2D-SFS, modeled 2D-SFS, residuals between the model and the data, and marginal SFS.

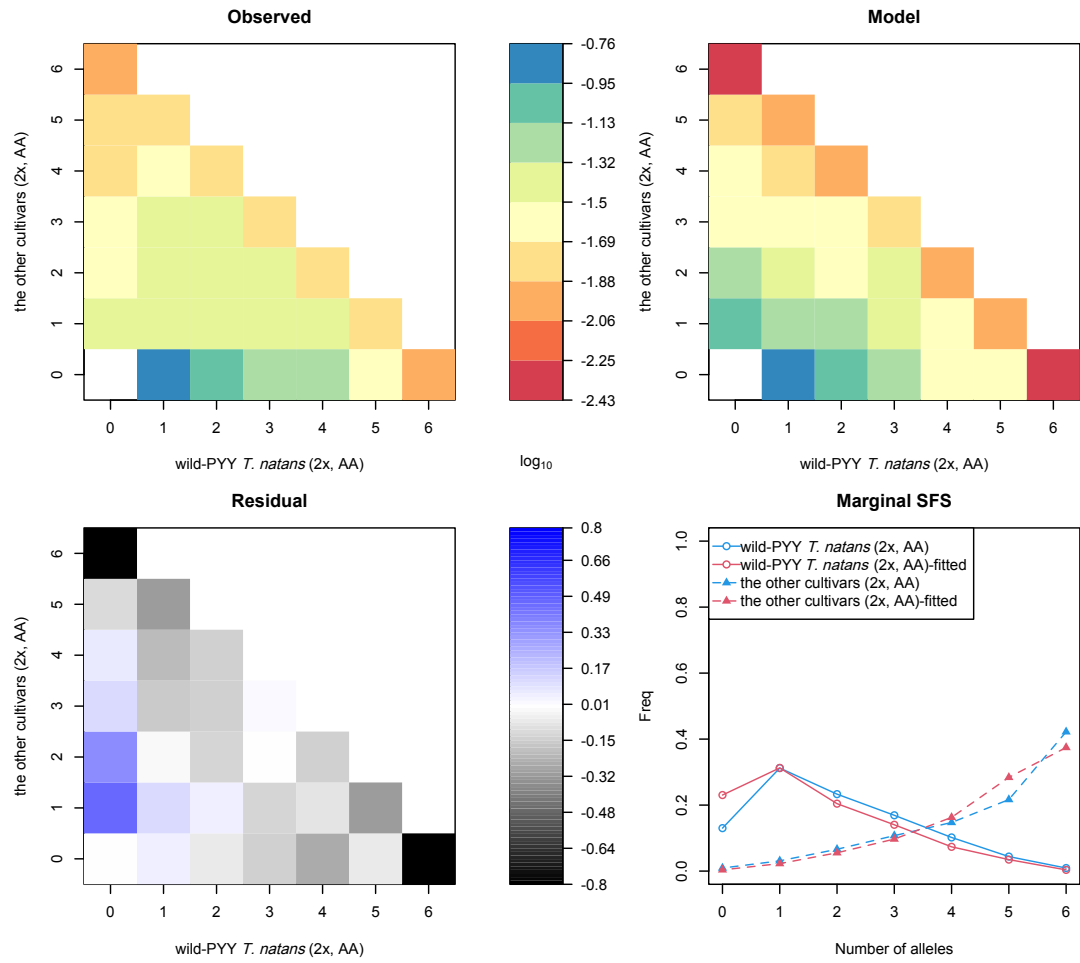


Figure S7 (continued)

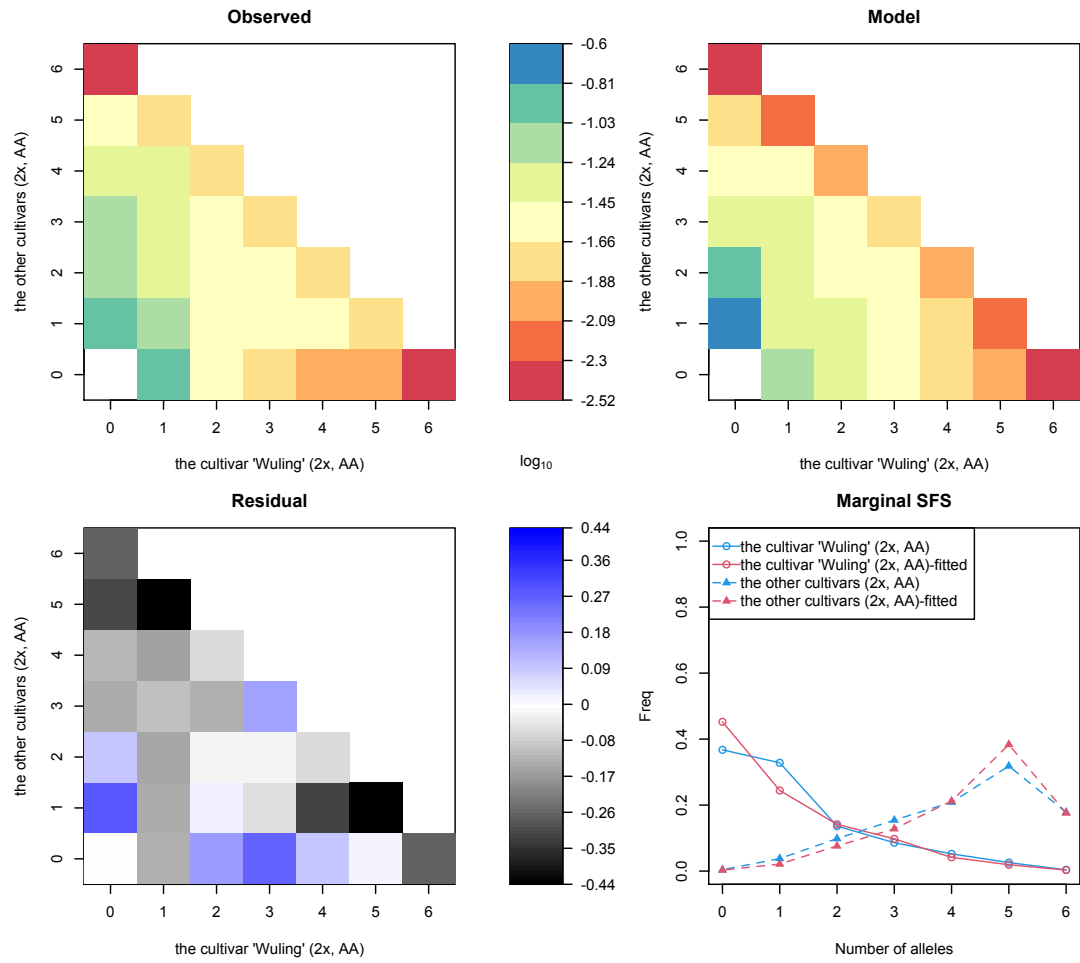


Figure S7 (continued)

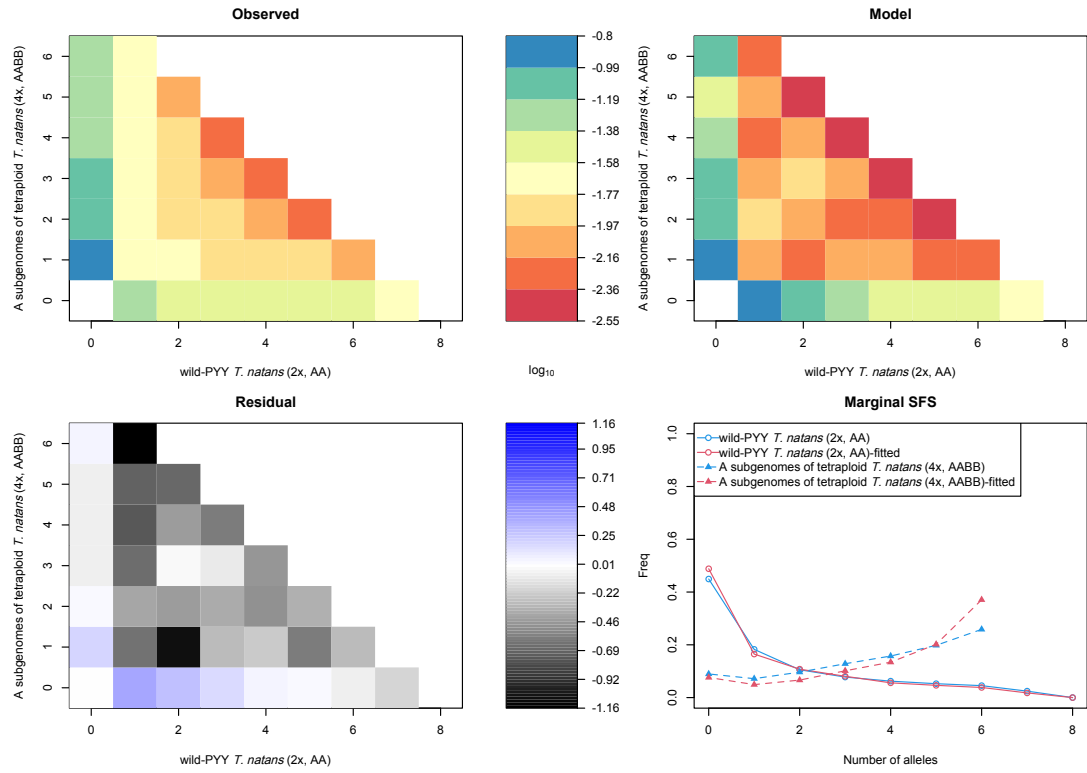


Figure S7 (continued)

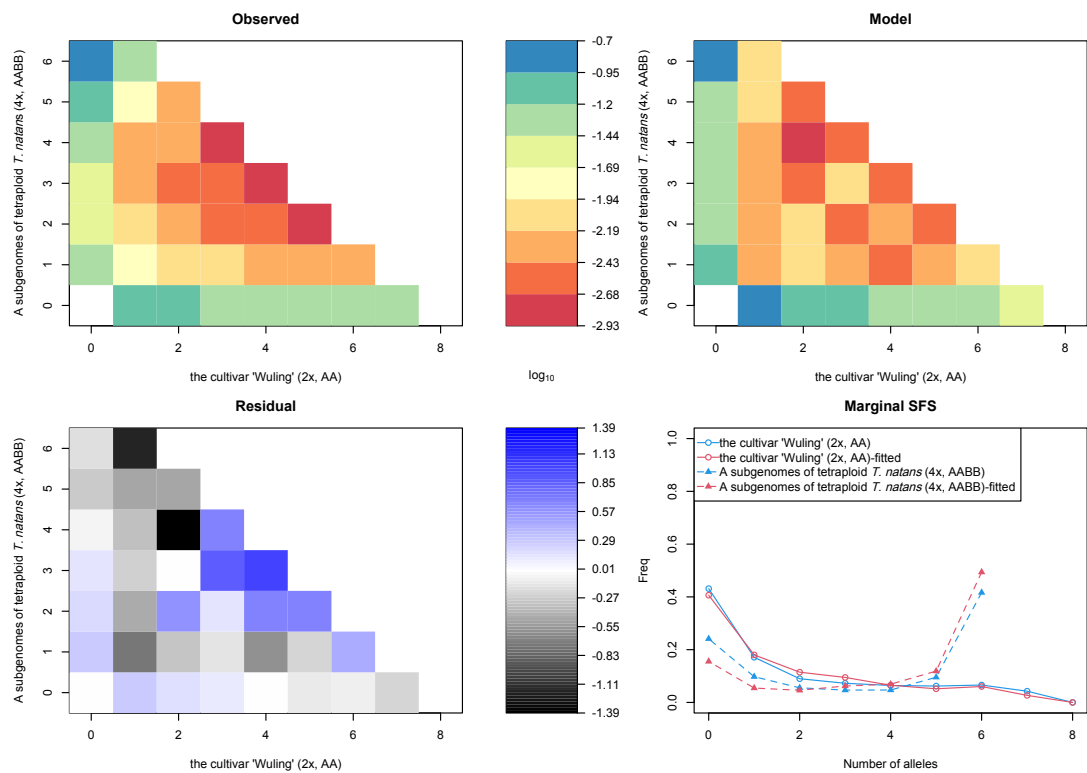


Figure S7 (continued)

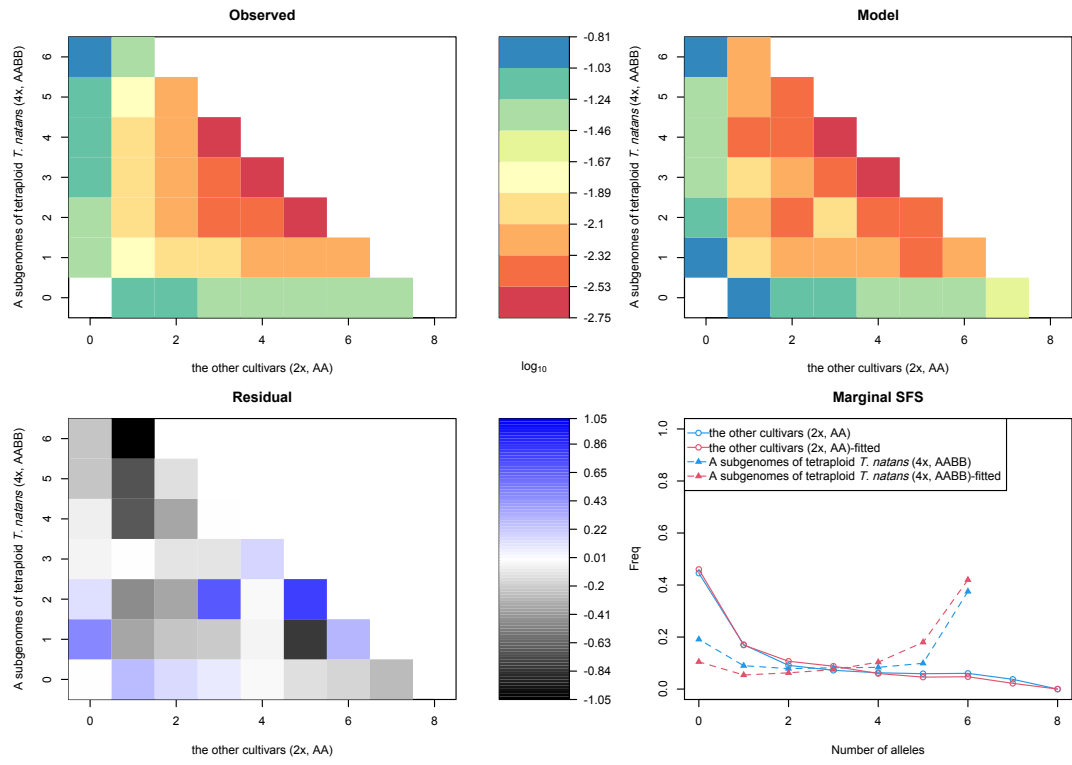


Figure S7 (continued)

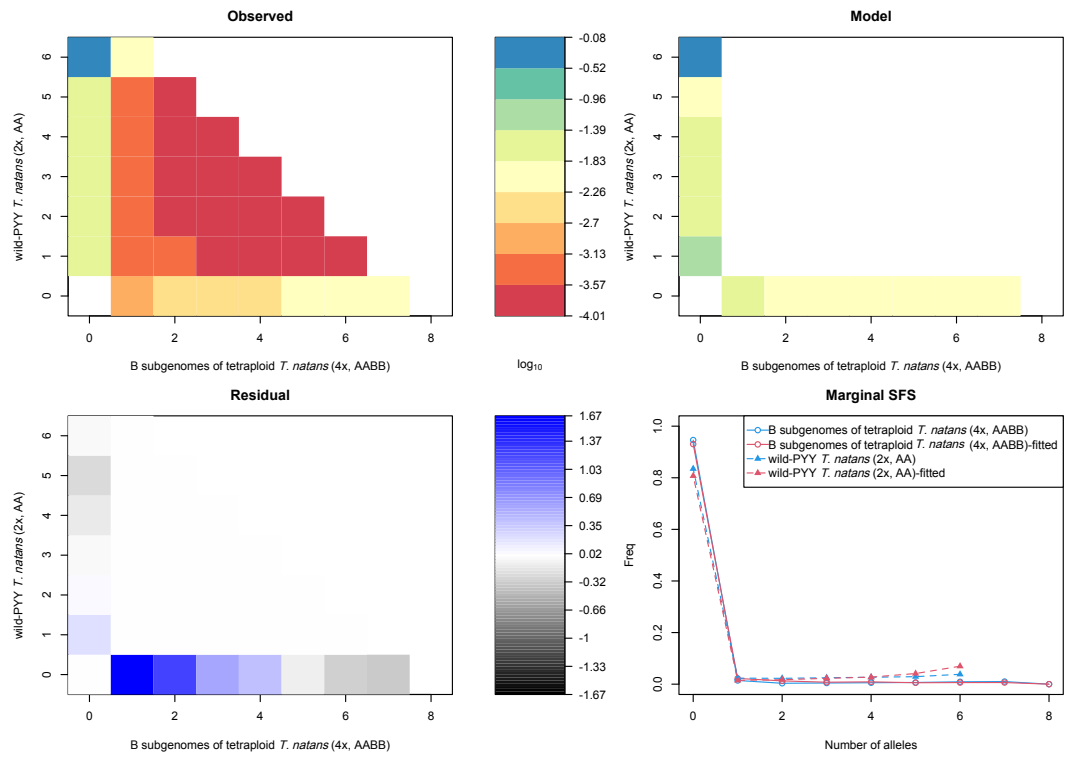


Figure S7 (continued)

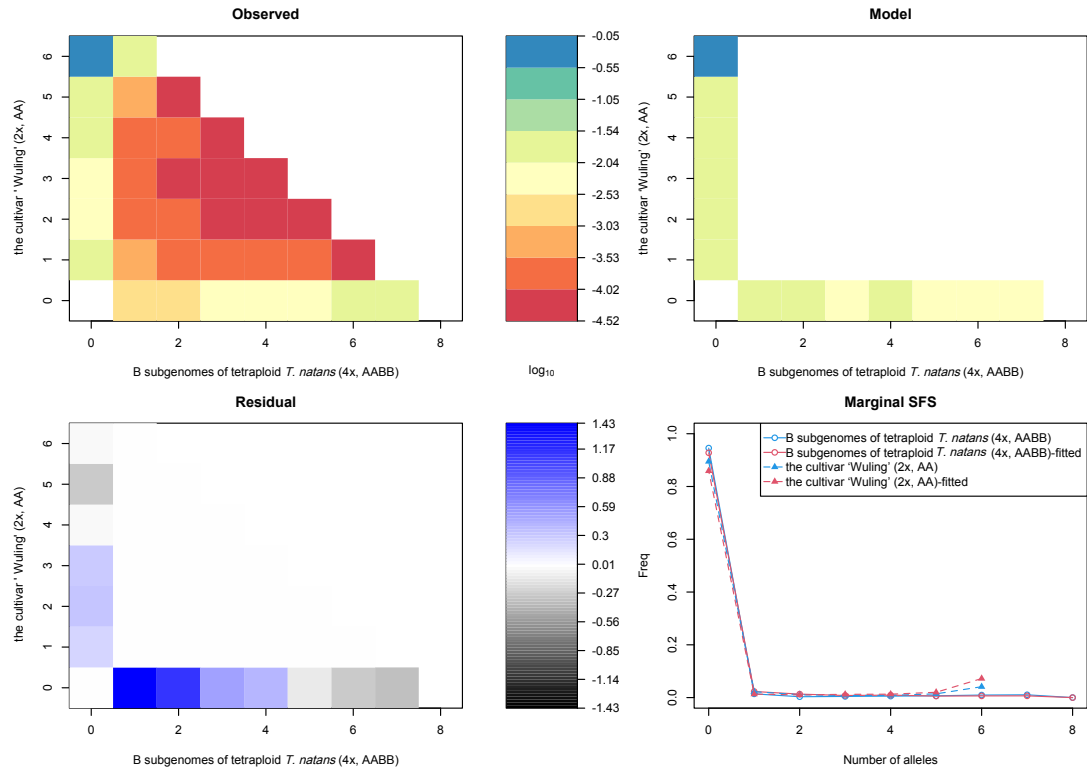


Figure S7 (continued)

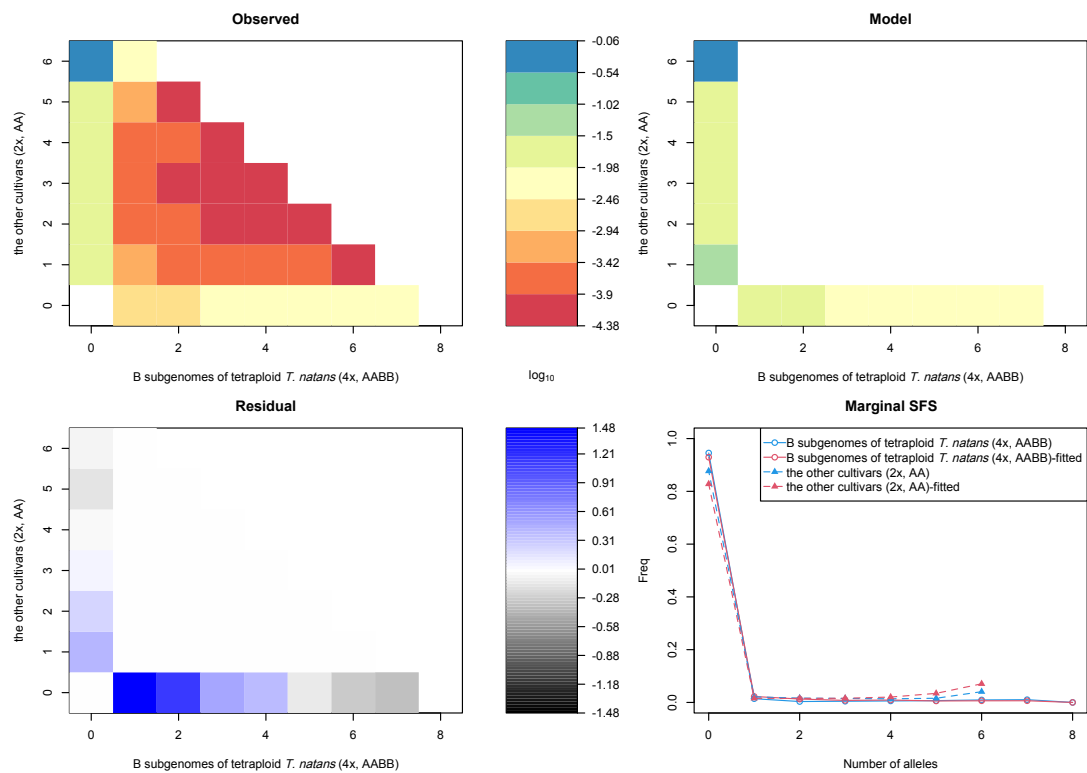


Figure S7 (continued)

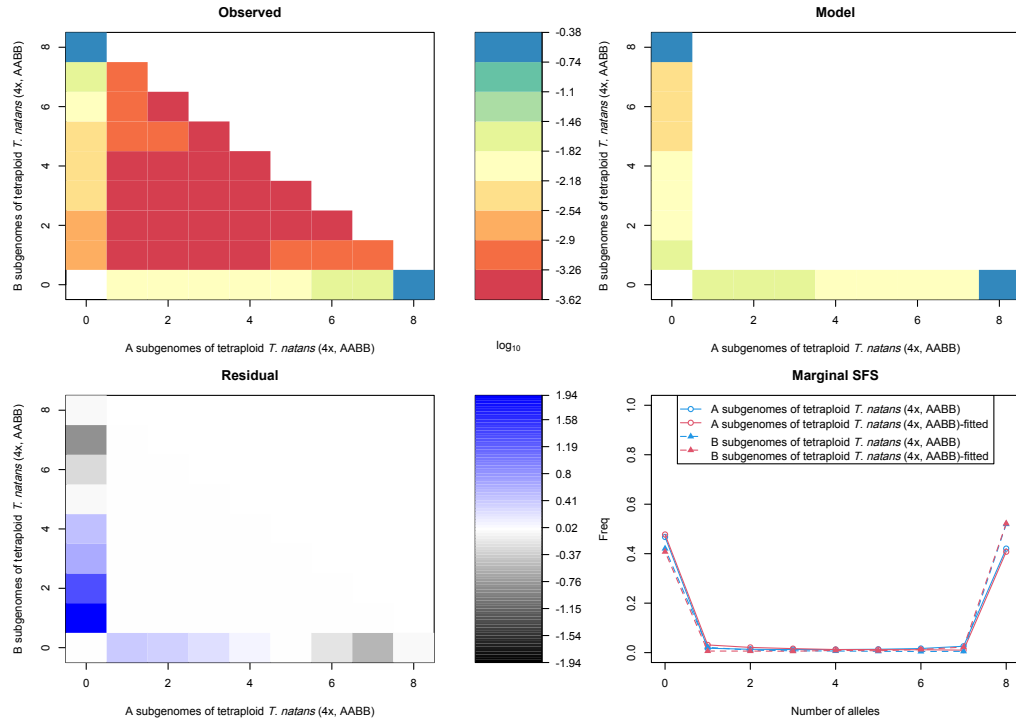


Figure S7 (continued)

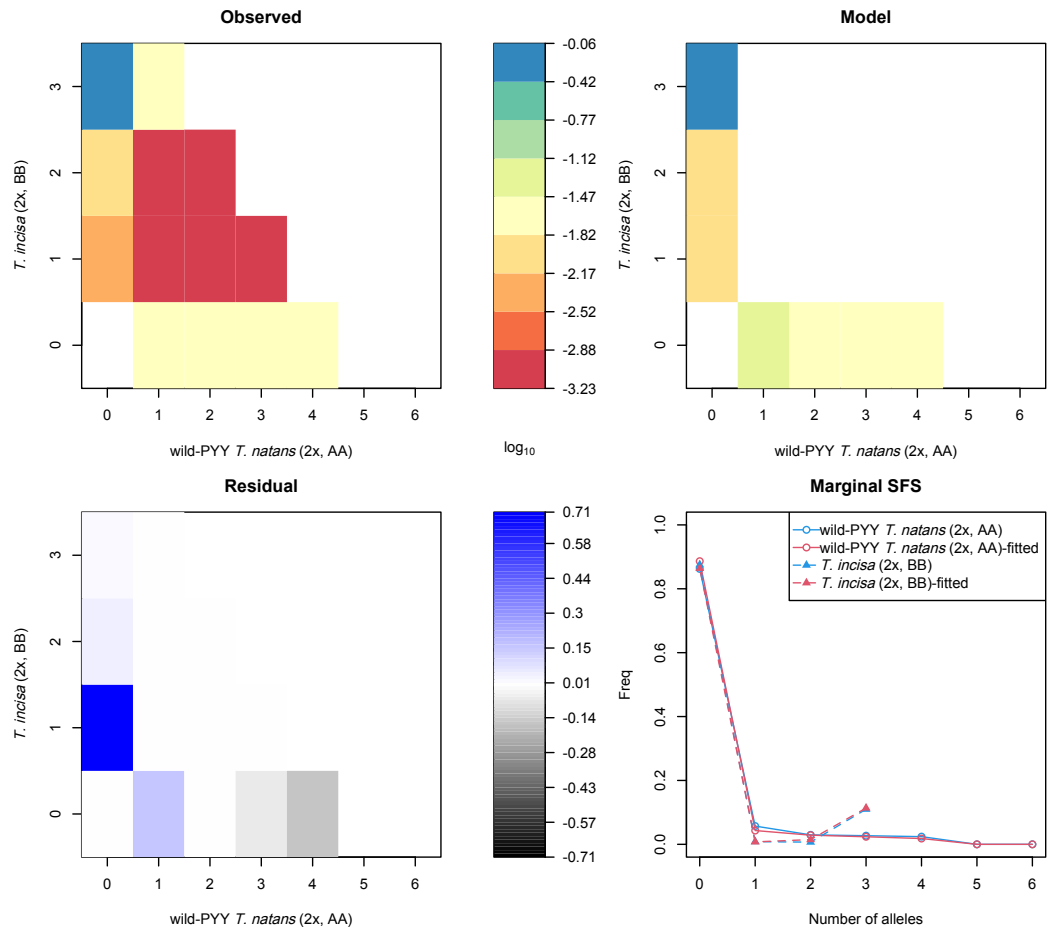


Figure S7 (continued)

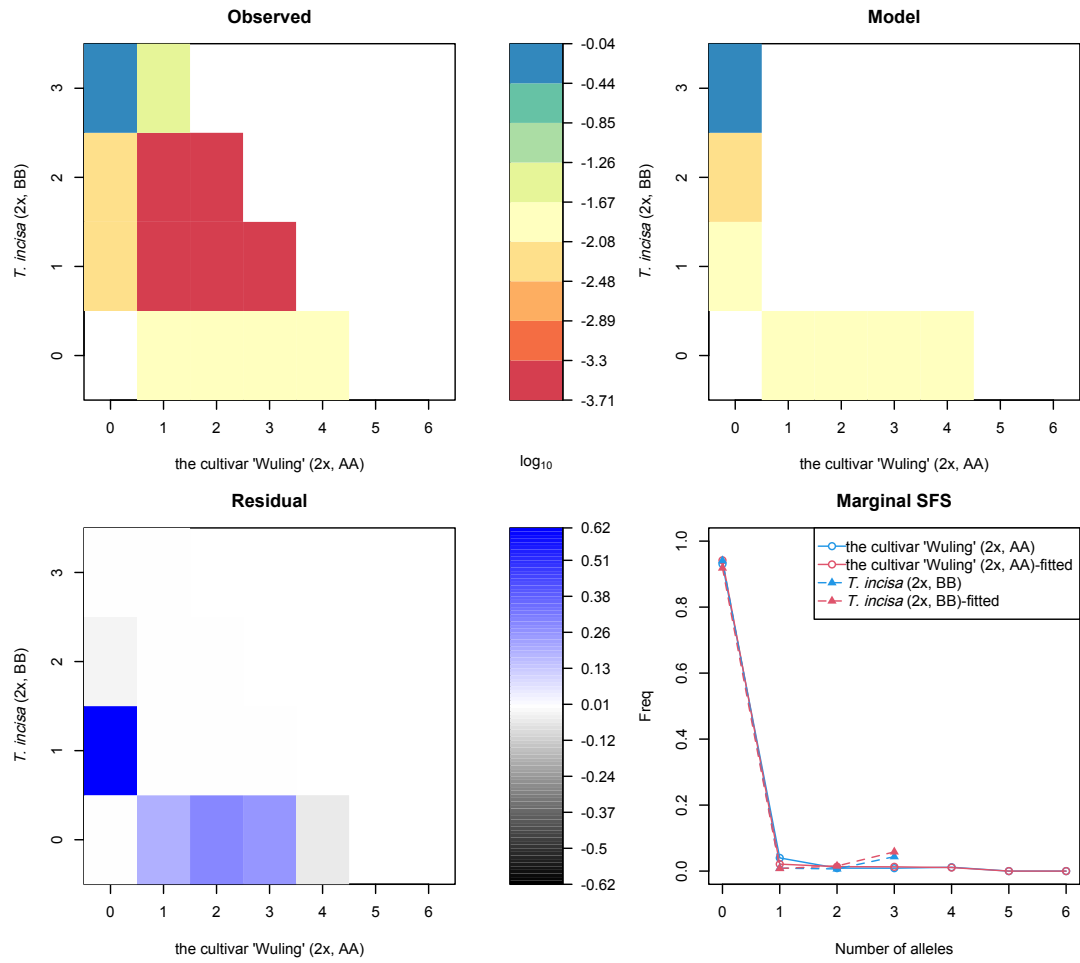


Figure S7 (continued)

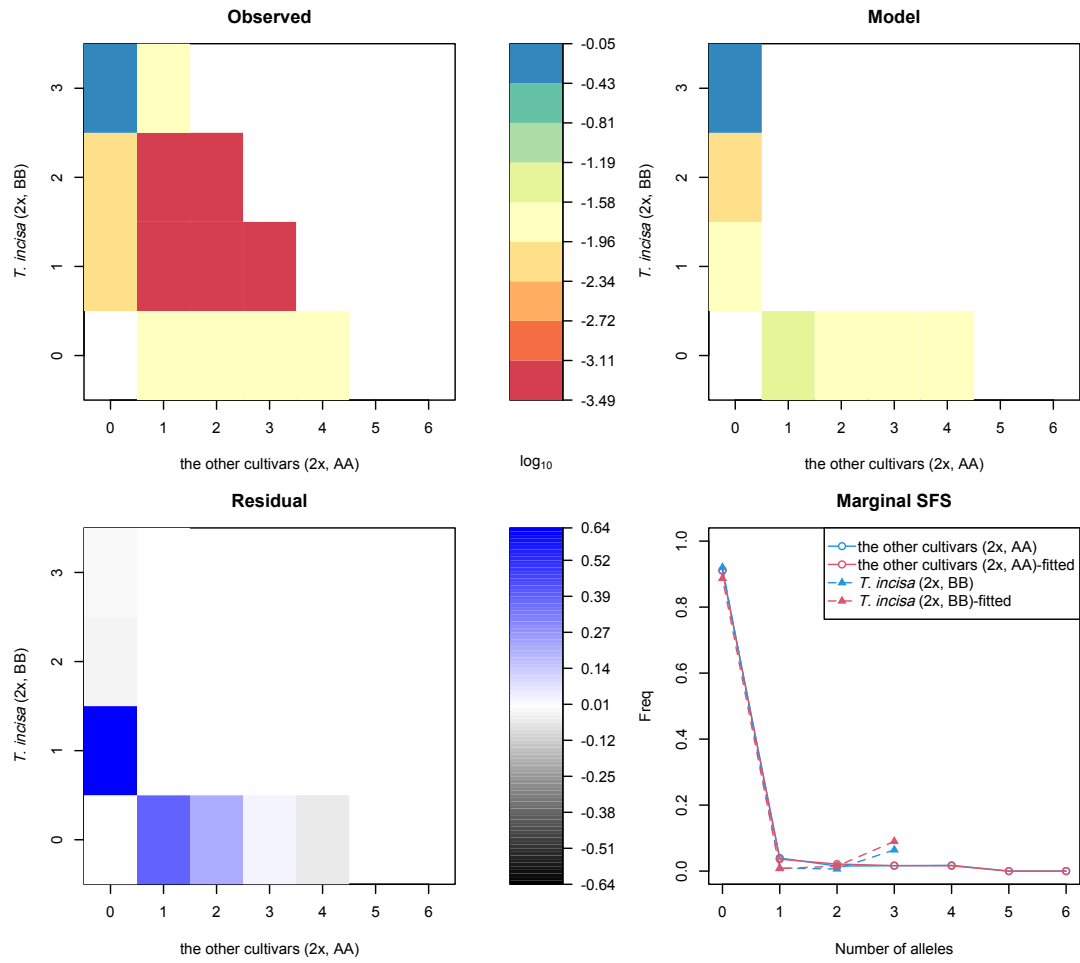


Figure S7 (continued)

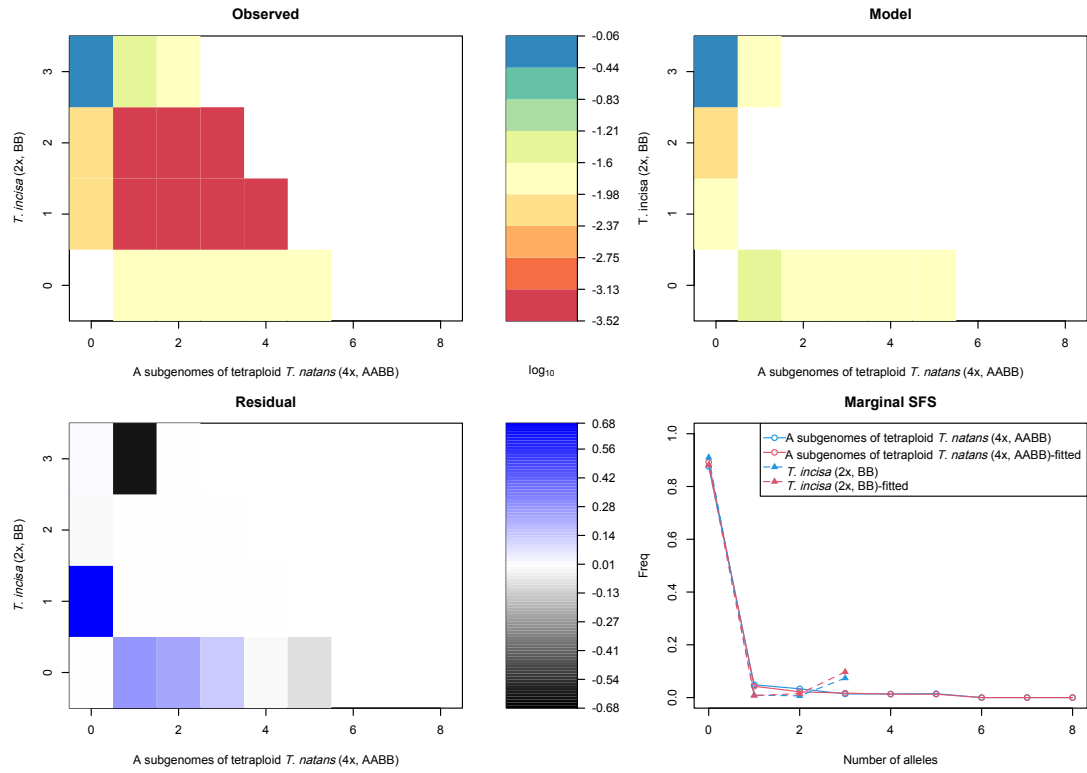


Figure S7 (continued)

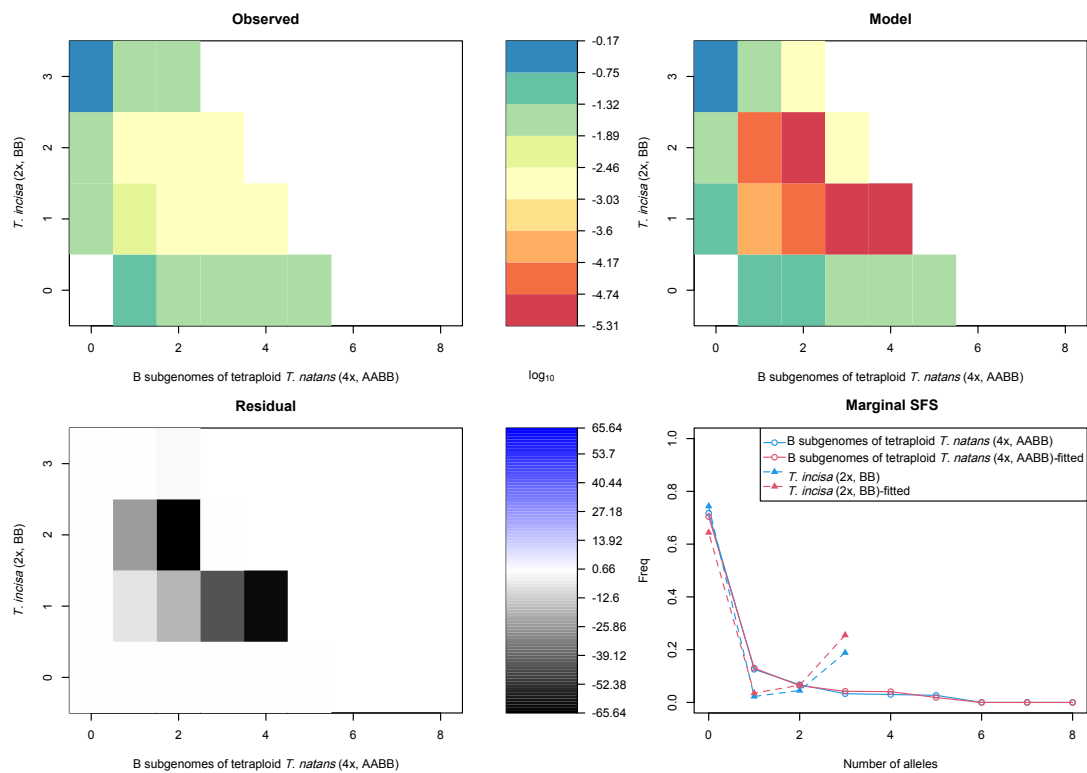


Figure S7 (continued)

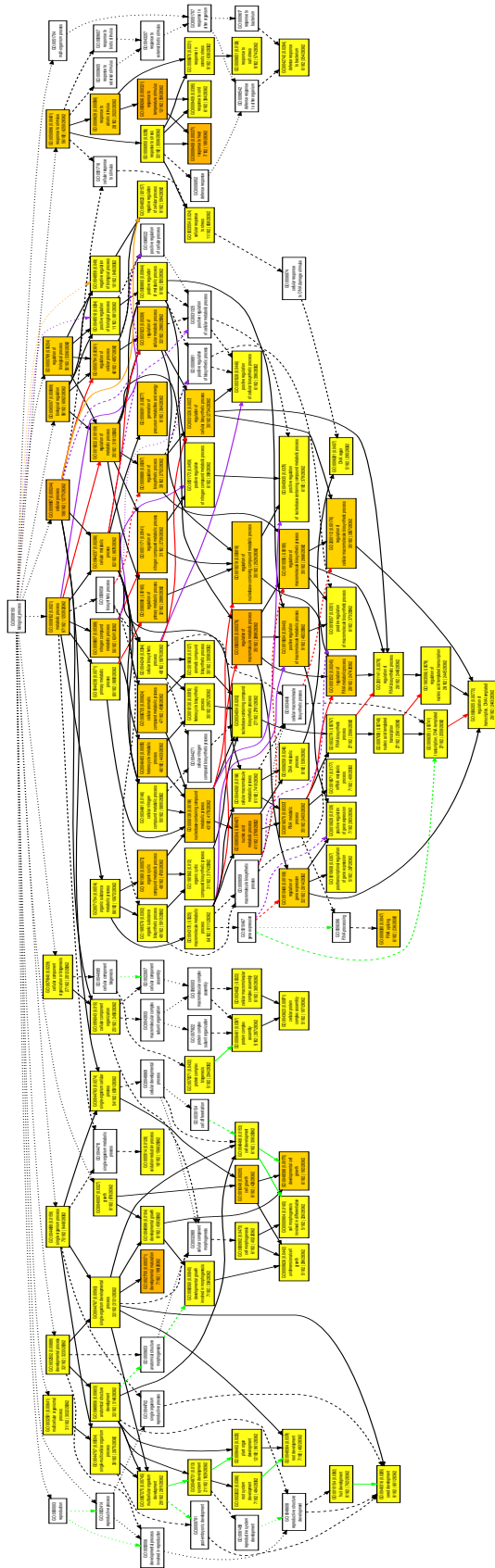


Figure S8 Significantly enriched biological process GO categories of 205 candidate genes under positive selection.

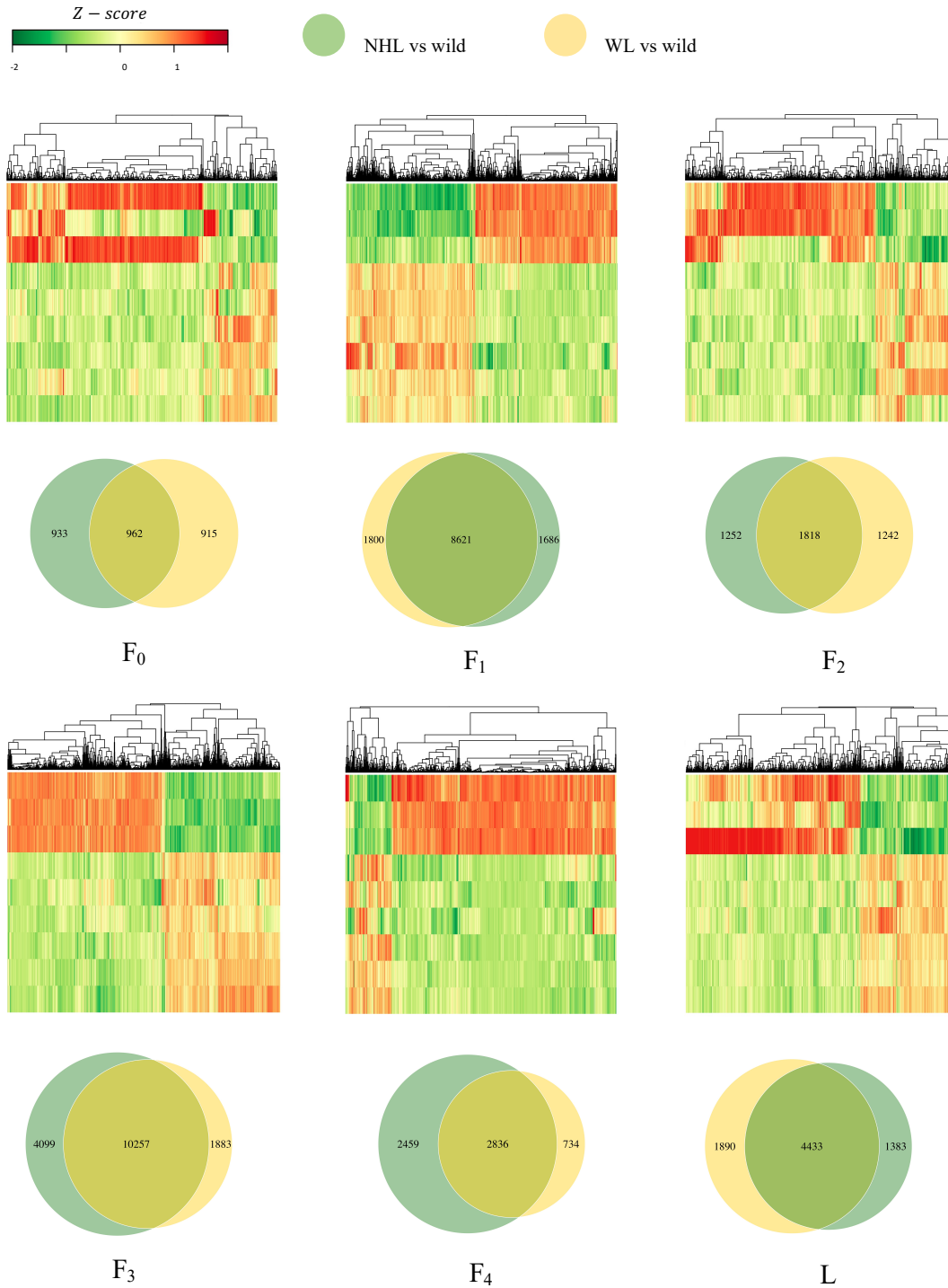


Figure S9 Heatmaps and Venn diagrams of common differentially expressed (up- or downregulated) genes (DEGs) shared by the two cultivar–wild comparisons (i.e. ‘Wuling’ vs. wild and ‘Nanhuling’ vs. wild). F₀: flower bud, F₁: fertilized flower, F₂: fruit before sepal abscission, F₃: fruit after sepal abscission, F₄: juvenile fruit, L: leaf.

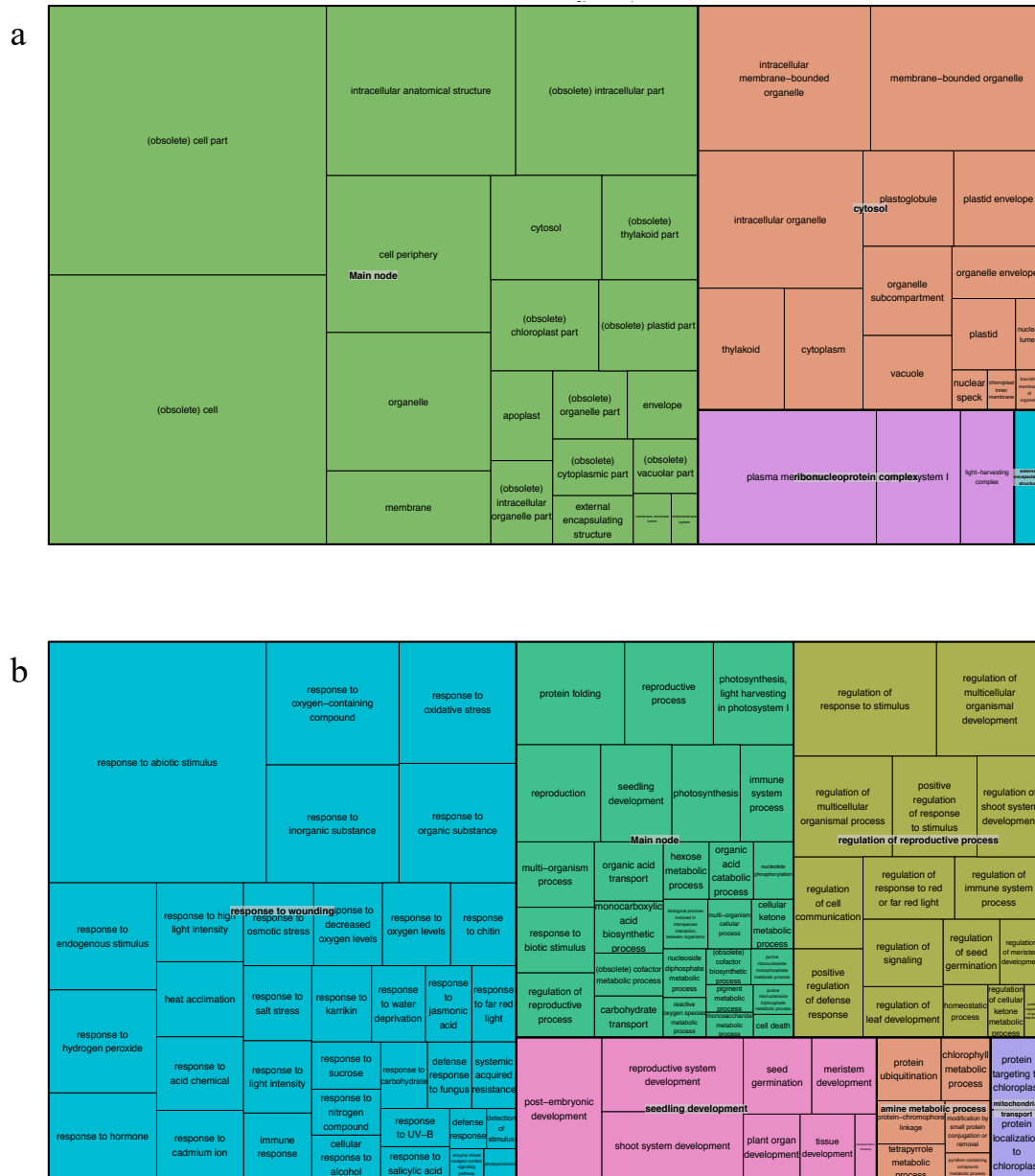


Figure S10 Significantly enriched GO categories under biological process of differentially expressed (up- or downregulated) genes (DEGs) shared by the two cultivar–wild comparisons (i.e. ‘Wuling’ vs. wild and ‘Nanhuling’ vs. wild). a, c, e, g, i, upregulated genes at developmental stages, F₀ (flower bud), F₁ (fertilized flower), F₂ (fruit before sepal abscission), F₃ (fruit after sepal abscission) and F₄ (juvenile fruit), and in leaf tissues, respectively. b, d, g, h, k, downregulated genes at F₀, F₁, F₂, F₃ and F₄ stages and in leaf tissues, respectively.

c

membrane invagination	response to UV-B	tropism	heterochromatin assembly	ribosomal small subunit assembly	cellular response to acid chemical	wax metabolic process	hormone transport	meristem development	shoot system morphogenesis	plant epidermis development					
flavonoid biosynthetic process	response to karrikin	response to gravity	regulation of stomatal movement	cell wall modification involved in multidimensional cell growth	stomatal movement	protein import into chloroplast stroma	DNA endoreplication	karyogamy	meristem maintenance	root system development	phloem or xylem histogenesis	gametophyte development			
cytokinesis by cell plate formation	regulation of flavonoid biosynthetic process	response to jasmonic acid	amino acid import	regulation of meristem structural organization	water transport	pyrimidine nucleoside biosynthetic process	histone H3-K9 methylation	asymmetric cell division	defense response by callose deposition	callose localization	anatomical structure arrangement	post-embryonic animal organ morphogenesis	plant epidermal cell differentiation	cellularization	
flavonoid metabolic process	positive regulation of flavonoid biosynthetic process	photoregulation	mitotic recombination	histone H3-K9 modification	response to sucrose	regulation of defense response to bacterium	pyrimidine biosynthetic process	regulation of DNA endoreplication	dsRNA processing	response to dsRNA	plant epidermis morphogenesis	embryo sac development	post-embryonic animal organ development	seed coat development	
response to nematode	heterochromatin organization	modulation by symbiont of RNA levels in host	cellular response to virus	protein nitrosylation	regulation of cell wall organization or biogenesis	regulation of response to alcohol	response to heat	response to salicylic acid	regulation of gene silencing	response to salicylic acid	maintenance of cell number	xylem development	syncytium formation	animal organ formation	phloem transport
response to cyclopentenone	muilage metabolic process	regulation of meristem development	fluid transport	cellular response to iron ion	defense response to insect	RNA secondary structure unwinding	regulation of response to osmotic stress	acclimation	gibberellin metabolic process	terpenoid metabolic process	stem cell population maintenance	stomatal complex patterning	cuticle development	vascular transport	cell fate specification

d

response to water deprivation	seed germination	response to jasmonic acid	meristem development	regulation of tetrapyrrole metabolic process	regulation of flower development	isoprenoid catabolic process	terpenoid catabolic process	response to gravity	sucrose biosynthetic process	response to monosaccharide	flavonoid biosynthetic process	seedling development	
phyllome development	response to karrikin	galactolipid biosynthetic process	post-embryonic animal organ development	heat acclimation	regulation of undimensional cell growth	alternative mRNA splicing, via spliceosomes	protein targeting to chloroplast	abscisic acid biosynthetic process	defense response by callose deposition in cell wall	histone H3-K9 modification	negative regulation of phosphoinositide signal transduction system	protein localization to chloroplast	
response to cadmium ion	regulation of response to red or far red light	starch metabolic process	response to salicylic acid	regulation of chlorophyll metabolic process	chloroplast RNA processing	regulation of phosphorelay signal transduction system	cell wall assembly	salicylic acid mediated signaling pathway	Golgi to vacuole transport	histone H3-K9 methylation	jasmonic acid and ethylene-dependent systemic response	very long-chain fatty acid biosynthetic process	
response to chitin	galactolipid metabolic process	flavonoid metabolic process	regulation of response to alcohol	stomatal closure	stomatal process	regulation of response to water deprivation	muilage metabolic process	regulation of actin filament-based process	dehiscence	regulation of shoot system morphogenesis	pollen germination	regulation of meristem development	
stomatal movement	regulation of stomatal movement	regulation of shoot system development	cuticle development	positive regulation of response to water deprivation	regulation of leaf development	induced systemic resistance	response to osmotic stress	regulation of response to osmotic stress	regulation of secondary metabolic process	regulation of root development	cellular response to dsRNA	seed maturation	seed dormancy process

Figure S10 (continued)

g

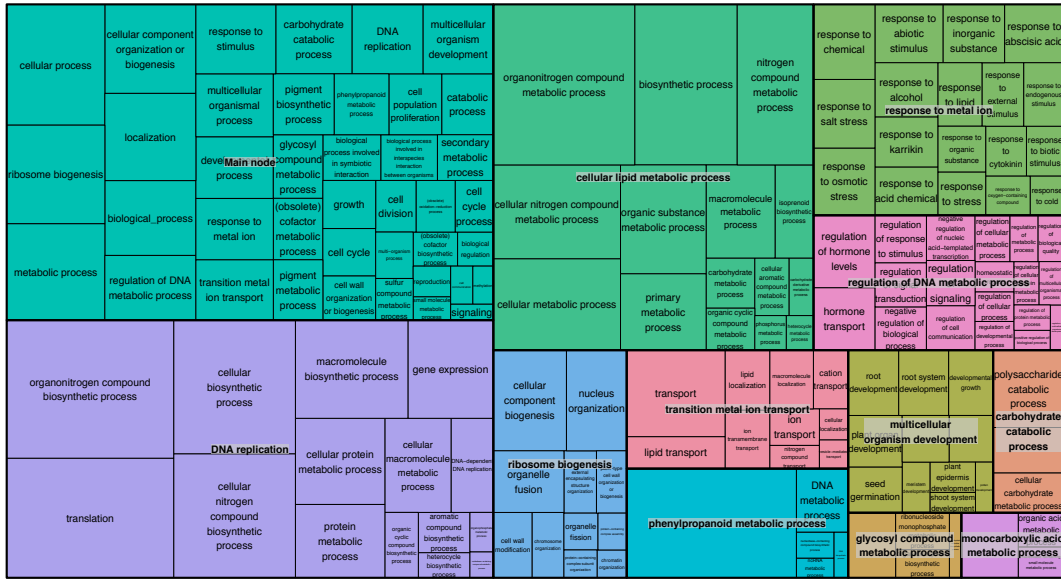
response to salt stress	root development	trichome differentiation	abscisic acid catabolic process	positive regulation of histone modification	positive regulation of post-embryonic development	postreplication repair	cuticle development	DNA endoreplication	positive regulation of defense response to bacterium	cell fate specification	jasmonic acid metabolic process		
	meristem development	plant-type cell wall biogenesis	seedling development	flavonoid metabolic process	positive regulation of multi-organism process	cytokinesis by cell plate formation	response to nematode	fluid transport	shoot system morphogenesis	water transport	isocitrate metabolic process	terpene metabolic process	
meristem maintenance		cellular response to acid chemical	regulation of meristem development	regulation of abscisic acid-activated signaling pathway	Main node	stomatal complex patterning	cell wall assembly	asymmetric cell division	mRNA transcription	syncytium formation	response to transition metal nanoparticle	regulation of stomatal movement	regulation of anthocyanin metabolic process
	plant epidermis development	response to UV-B	maintenance of cell number	regulation of response to alcohol	cell wall modification involved in multidimensional cell growth	flavonoid biosynthetic process	photosynthesis	asymmetric cell division	mitotic recombination	response to disaccharide	regulation of multi-organism process	oxylipin metabolic process	response to ozone
gametophyte development		anatomical structure arrangement	RNA secondary structure unwinding	post-embryonic animal organ development	defense response to Gram-negative bacterium	membrane invagination	histone H3-K9 methylation	regulation of shoot system development	brassinosteroid homeostasis	starch metabolic process	dehiscence	pollen germination	regulation of gene silencing

h

response to salicylic acid	vegetative to reproductive phase transition of meristem	salicylic acid mediated signaling pathway	seed germination	entrainment of circadian clock	negative regulation of phosphorelay signal transduction system	desubstrin-independent cleavage of nuclear-histonebound mRNA	nuclear-histonebound mRNA catabolic process	cellular response to dsRNA	regulation of anion channel activity	regulation of leaf development	meristem development			
	response to chitin	energy quenching	heat acclimation	response to transition metal nanoparticle	regulation of meristem development	longitudinal axis specification	regulation of auxin mediated signaling pathway	regulation of photosynthesis	fat-soluble vitamin metabolic process	pollen germination	regulation of leaf morphogenesis	cuticle development		
regulation of response to red or far red light		response to karrikin	nonphotochemical quenching	regulation of chlorophyll metabolic process	stomatal closure	protein targeting to chloroplast	regulation of leaf senescence	regulation of anthocyanin metabolic process	histone H3-K9 modification	phloem or xylem histogenesis	response to ozone	cellular zinc ion homeostasis	defense response by callose deposition	animal organ senescence
	regulation of shoot system development	stomatal movement	response to sucrose	flavonoid metabolic process	transduction Main node	chloroplast RNA processing	response to freezing	regulation of flavonoid biosynthetic process	mitotic recombination	xanthophyll metabolic process	regulation of gibberellin acid mediated signaling pathway	auxin transport	induced systemic resistance	meristem maintenance
response to jasmonic acid		seedling development	anthocyanin-containing compound metabolic process	systemic acquired resistance	wax biosynthetic process	response to singlet oxygen	positive chemotaxis	photosynthesis	pectin biosynthetic process	pigment catabolic process	response to nitric oxide	phloem or xylem histogenesis	response to ozone	cellular zinc ion homeostasis

Figure S10 (continued)

i



j

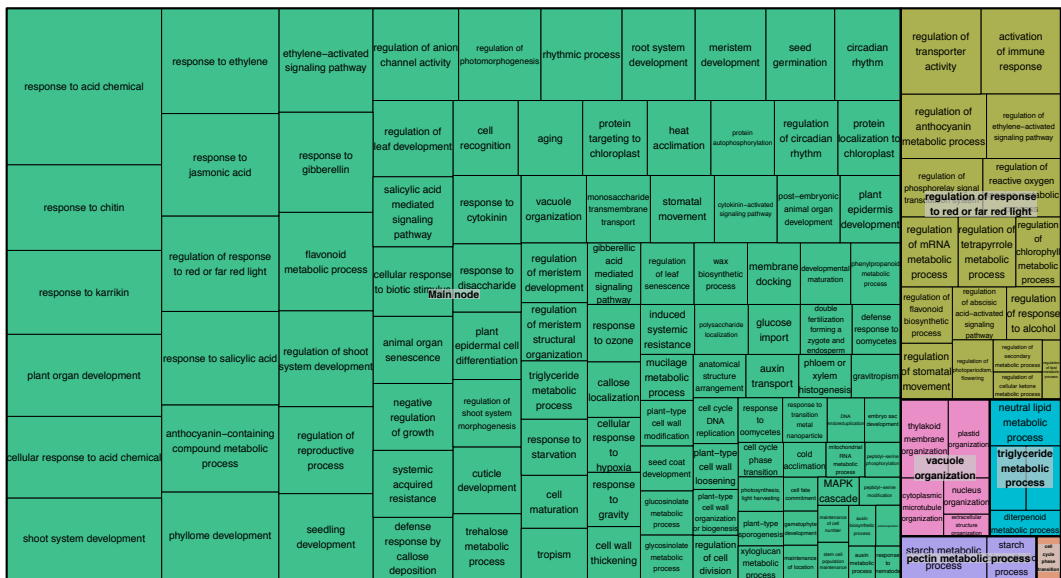
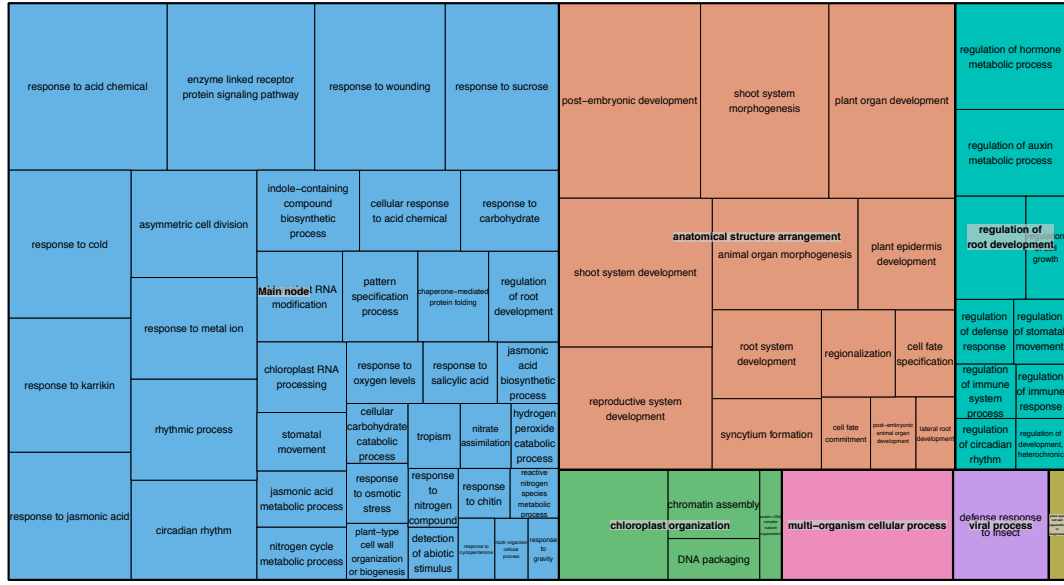


Figure S10 (continued)

k



l

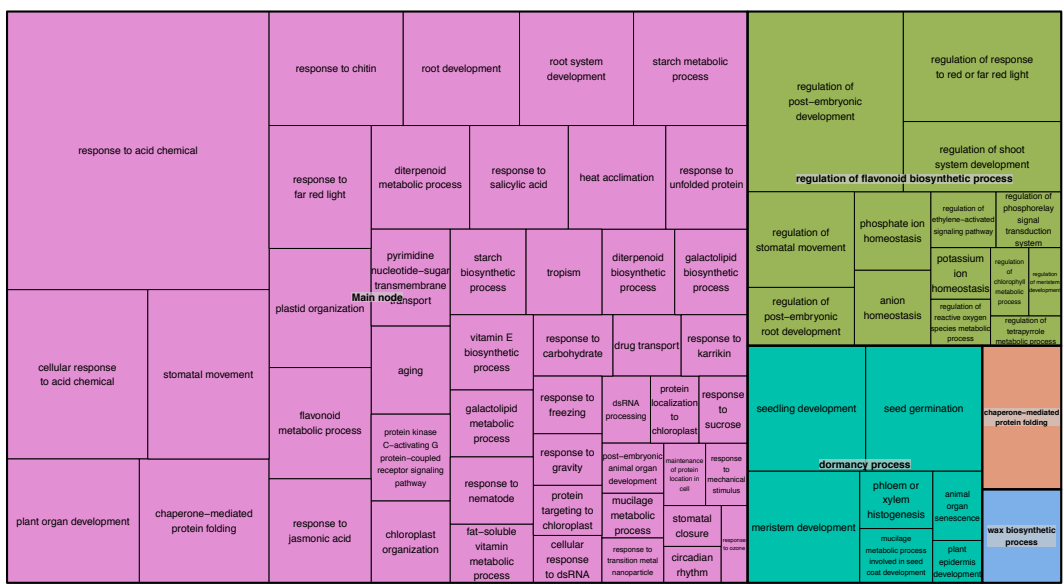
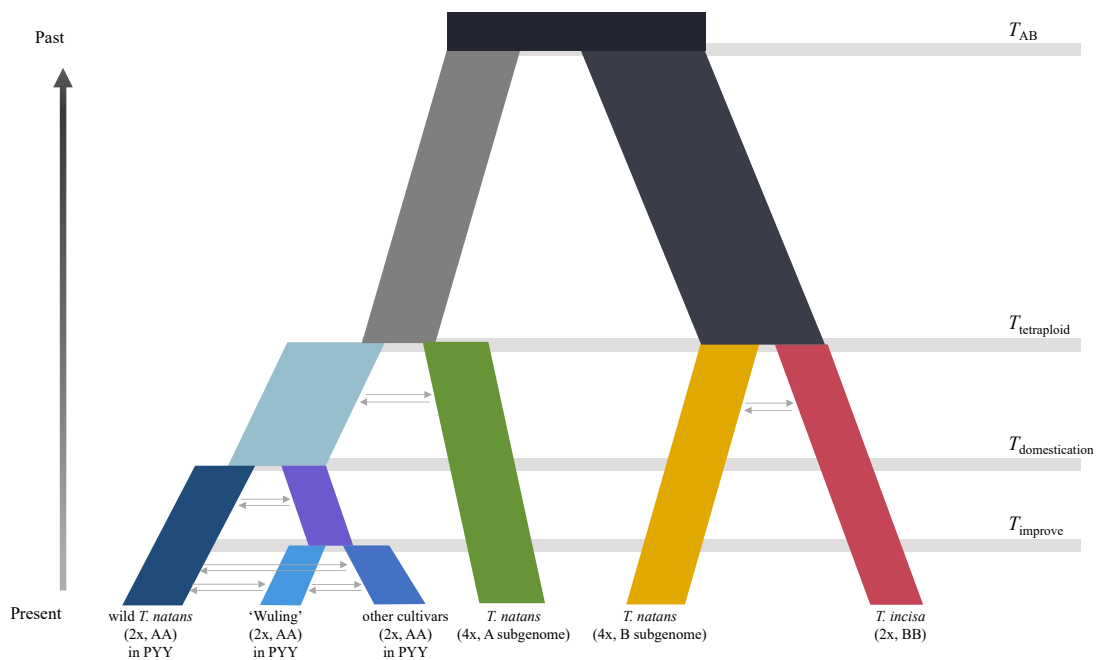
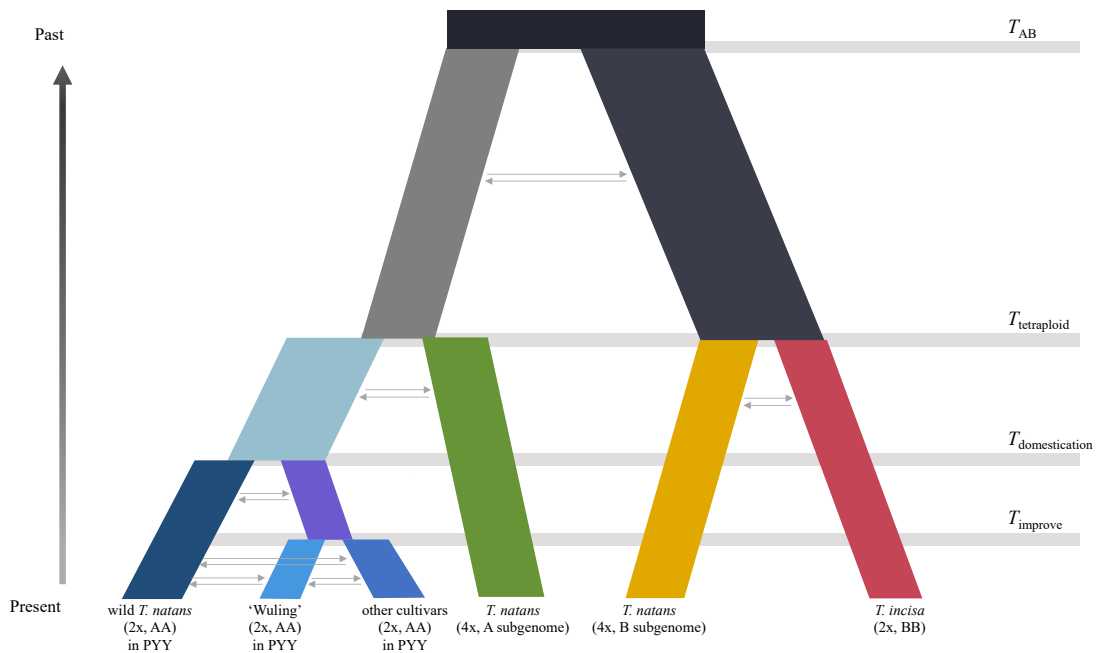


Figure S10 (continued)

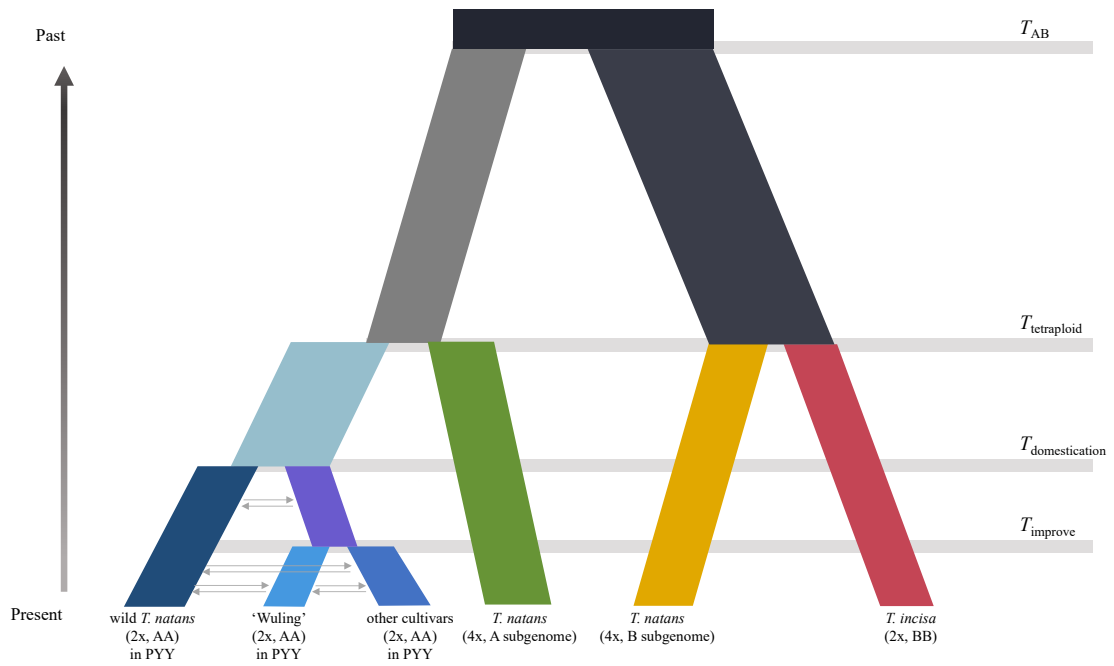


Model I

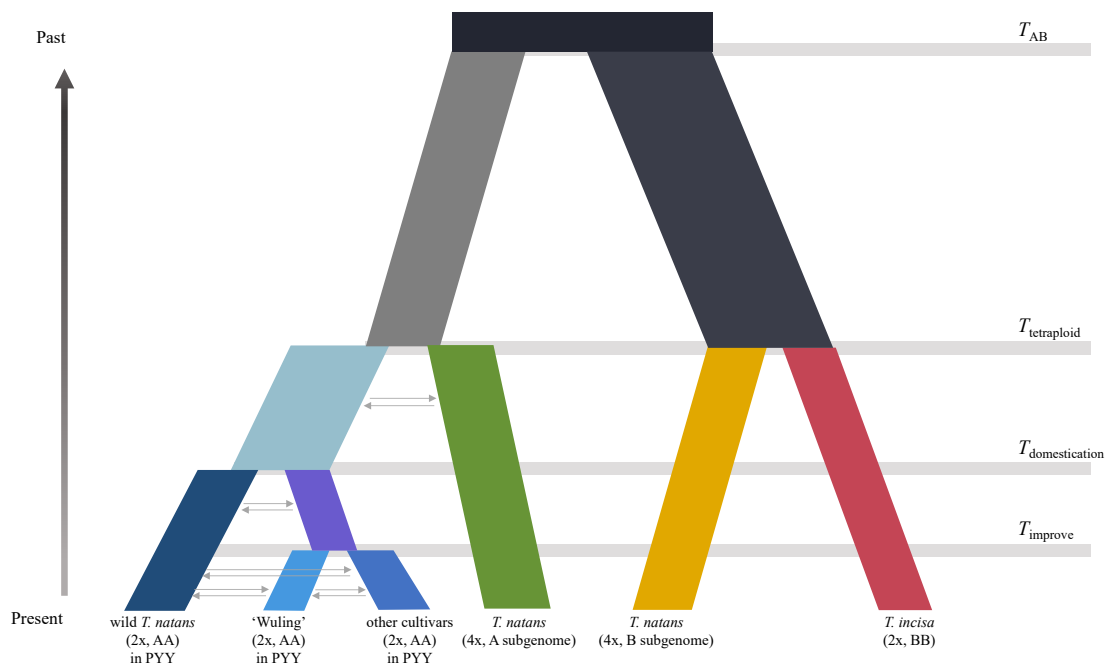


Model II

Figure S11 Test of alternative demographic models, with different sets of migration directions using FASTSIMCOAL2. Parameter abbreviations: T_{improve} , time of improvement event for *T. natans* cultivar 'Wuling'; $T_{\text{domestication}}$, time of domestication event for all cultivars of *T. natans*; $T_{\text{tetraploid}}$, time of origin of allotetraploid *T. natans* (4x, AABB); T_{AB} , divergence time of diploid *T. natans* and *T. incisa*.



Model III



Model IV

Figure S11 (continued).

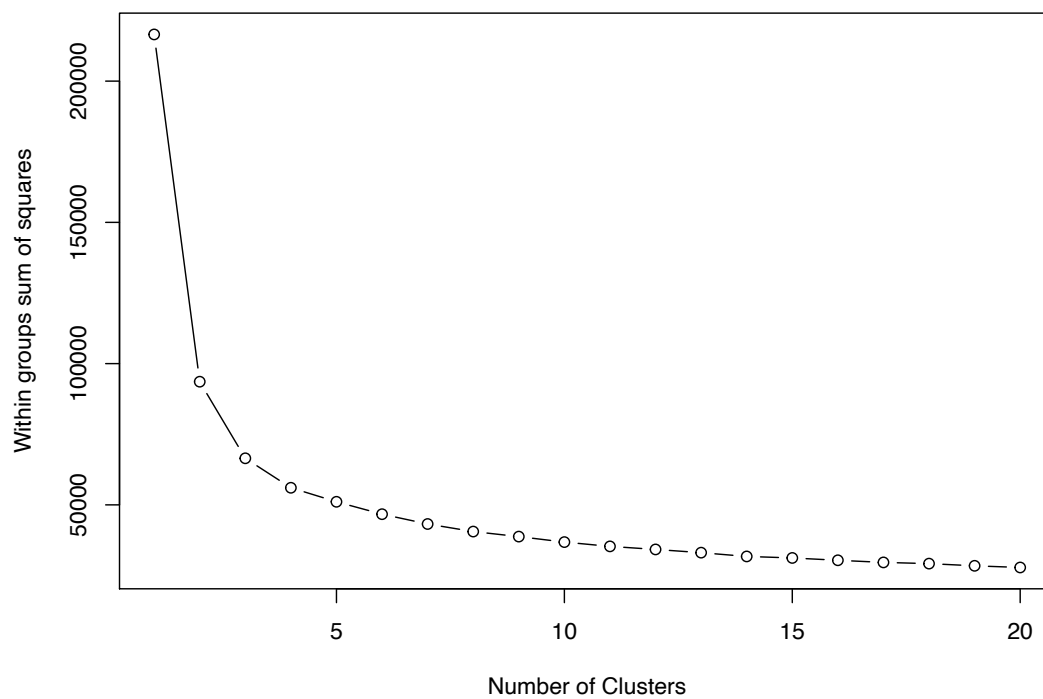


Figure S12 The relationship between the sum of squared error (SSE) and the number of clusters. The number of clusters was set from 1 to 20.